Response to the Comments from Referee #1

We sincerely thank the reviewer for the valuable feedback that we have used to check our newly-developed algorithm and improve the quality of our manuscript as well. The reviewer comments are laid out below in *italicized font* and specific concerns have been numbered. Our response is given in normal font.

This paper presents measurements from a lidar, ceilometer and sodar at Cape Grim, from which the boundary-layer height is derived. Although Cape Grim is an interesting station for measurements of pristine Southern Ocean air, it is not clear to me what the purpose of this paper is meant to be. Most of the results show three case studies which are little more than examples – they don't lead to any useful conclusion beyond this particular dataset.

At the heart of the difficulties encountered in this paper, and not discussed at all in the introduction, is what is meant by the BLH over the ocean and how this relates to the distribution of aerosols. The BLH is essentially a thermodynamic concept, but the marine boundary layer can be stable, inhibiting the vertical transport of aerosol. To affect a meaningful comparison with WRF, for example, one would need to understand what WRF means by BLH and whether that is relevant to the distribution of aerosols (i.e. are they likely to be mixed throughout the BL or confined to low levels by inversions in the temperature profile?). The issue is compounded here by the very different 'BLH' derived from the two remote sensing instruments, strongly suggesting that a simple definition is inappropriate.

Main comments

Regarding the conclusions of the paper:

1. You shouldn't validate measurements against a model!

Response: Thank you for the comments. In our revised version, we included the ERA5 reanalysis product, as an additional and straightforward check on our observations and WRF. Unfortunately, no radiosonde was launched for this campaign. We have added Figure 4, Figure 5 for statistical analysis of the whole observing period and re-plotted Figure 9, 10 and 11(now presented as Figure 10,11 and 12 in the revised version). Figure 4, Figure 5 and Figure 10-12 are shown as follows.

BLH comparison against ERA5 reanalysis data

The inter-comparison 1-h averaged BLHs for the miniMPL and ceilometer against ERA5 during the whole observing period are presented in Figure 4. For miniMPL, an excellent concordance is found between IEDA- and ERA5- derived BLHs, with a correlation coefficient of 0.78 (Figure 4a). The gradient method underestimates the BLH with largest negative bias of 0.83 km, though its coefficient value is slightly lower (0.71 in Figure 4b). It is probably because the gradient estimates appear to detect the largest negative gradient from the bottom-up. Similar to the miniMPL, the ceilometer generally provides lower BLHs compared to the ERA5, though some unidentified elevated aerosol layers result in a few points with much higher BLH than ERA5-BLH. However, the gradient method (Figure 4d) outperforms (Pearson's r = 0.50) the IEDA (Figure 4c, Pearson's r = 0.41) against ERA5 BLHs. The discrepancy and uncertainties between the miniMPL/ceilometer and ERA5 can be mainly attributed to (1) the different definitions of the BLHs applied to each method (i.e. edge/gradient detection from aerosol back-scattered signal for miniMPL/ceilometer, bulk Richardson method for ERA5), (2) the different air masses for the spatial separation of the observing sites, (3) the coarse resolution of ERA5 and (4) the presence of the lofted layer or cloud layers. Therefore, no single approach can cover all situations over this campaign. Among these causes, (1) (2) and (3) would influence our whole period. More details could be found in the section 3.2.1 of the revised version.

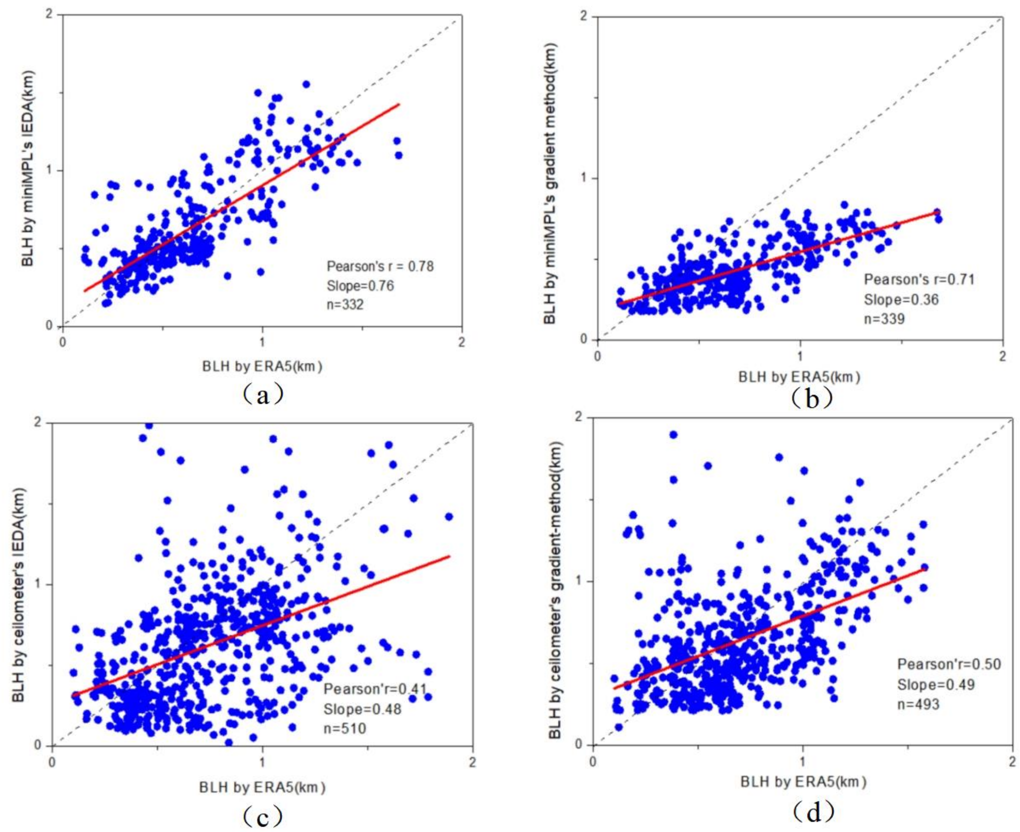

Figure 4. Comparison of 1-h averaged BLH estimations based on different instruments and

methods against ERA5 results: (a) IEDA from miniMPL (b) the gradient method from miniMPL (3) IEDA from the ceilometer and (4) the gradient method from the ceilometer. In each case, a linear regression through the origin is performed (red line) and statistics are shown: slope, Pearson’s linear correlation coefficient (Pearson’s r), slope, and number of samples (n). The black dashed line is a 1: 1 line.

Diurnal cycle of BLH

Considering the comparison in Figure 4 above, we chose IEDA for miniMPL and gradient method for ceilometer respectively to investigate the diurnal cycles of BLH (Figure 5). Generally, the ERA5 presents smoother and higher averaged BLHs (0.71±0.08 km) than those from miniMPL (0.64±0.06 km) and ceilometer (0.65±0.07 km). However, the diurnal cycles of BLH from 1 h-averaged miniMPL (IEDA) observations show good agreement with those from ERA5, especially from the early morning to 11:00 LST, with a negative bias (- 0.02 to -0.10 km). The miniMPL (IEDA) BLHs reached the maximum of 0.76 km at 14:00 LST while the ERA5 BLHs peaked at 0.86 km at 15:00 LST. In comparison, the ceilometer (gradient) shows more variable BLHs, as expected due to multiple sharp gradients corresponding to multi-layer or lofted aerosol layers, and presents less diurnal characteristic of MBL (marine boundary layer). Its BLH fluctuated from 0.52 to 0.72 km in the morning and appeared to collapse immediately afterward before growth at 19:00 LST again. The largest difference between miniMPL/ceilometer and ERA5 occurs during the MBL developing period (from 12:00 to 20:00 LST) and the mean nocturnal boundary layer are higher than 0.5 km.

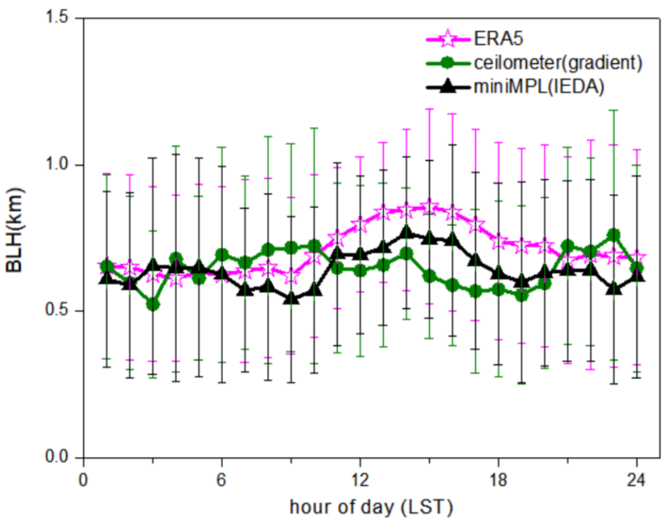

Figure 5. Resulting BLH for the whole observing period with 1-h averages from miniMPL (IEDA), ceilometer (gradient method) and ERA5. ERA5-estimated BLHs are shown as magenta stars.

We also replotted the BLH comparison, adding ERA5 reanalysis data and WRF model. Here only the plots of three case studies are presented in Figure 10-12. More details about the BLH comparison and MBL characteristic can be found in the section 3.2 of the revised version.

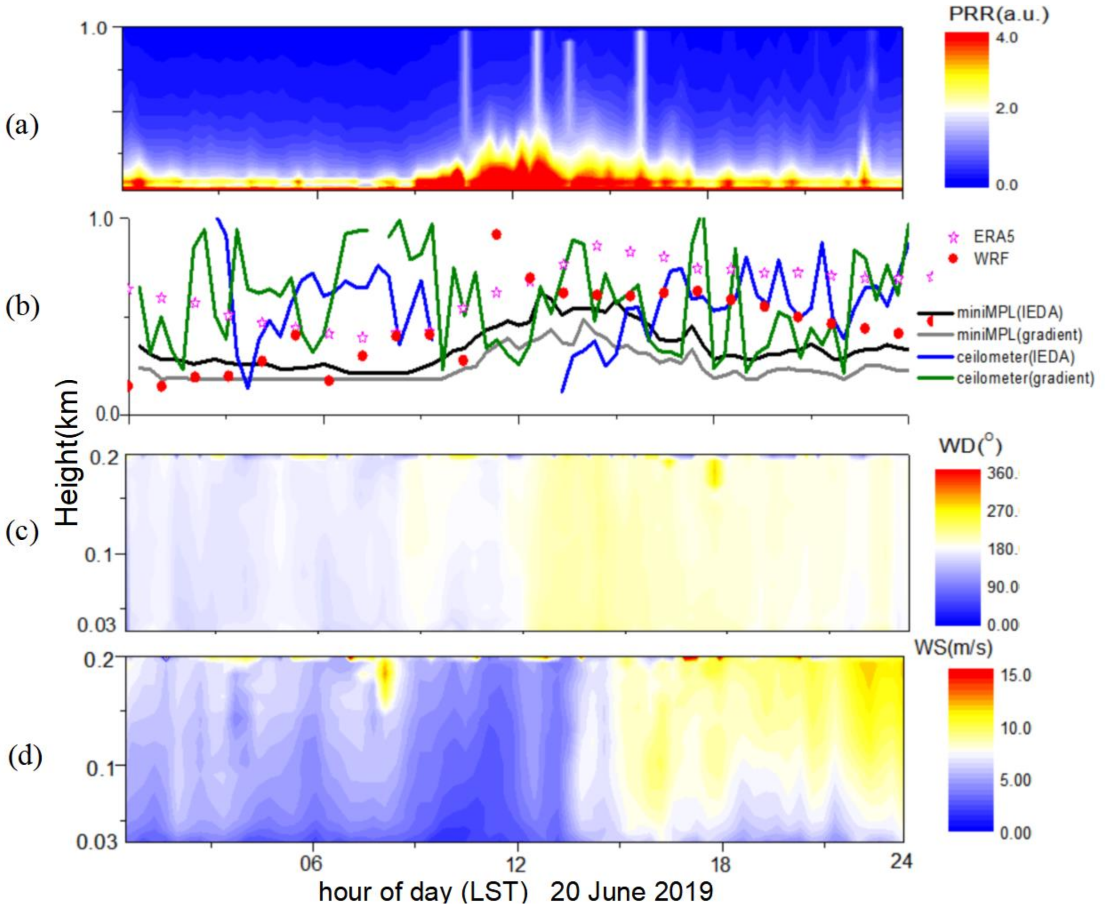

Figure 10. An example illustrating the retrieval of BLH using the lidar measurements obtained on 20 June 2019 over the Cape Grim observatory. The heights in all panels are in km AGL. (a): The normalized lidar backscattered signal using the miniMPL. The vertically aligned color bar (on a linear scale) on the right indicates the intensity in arbitrary units (a.u.). (b) Black lines， gray lines, blue lines and green lines indicate the 20-min averaged BLH estimations from the miniMPL (IEDA), miniMPL (gradient), ceilometer (IEDA) and ceilometer (gradient), respectively. The magenta star and red circles indicate the 1-h BLH results from the ERA5 reanalysis and WRF model. (c): wind direction(^{o}) and (d): wind speed (m/s) from sodar.

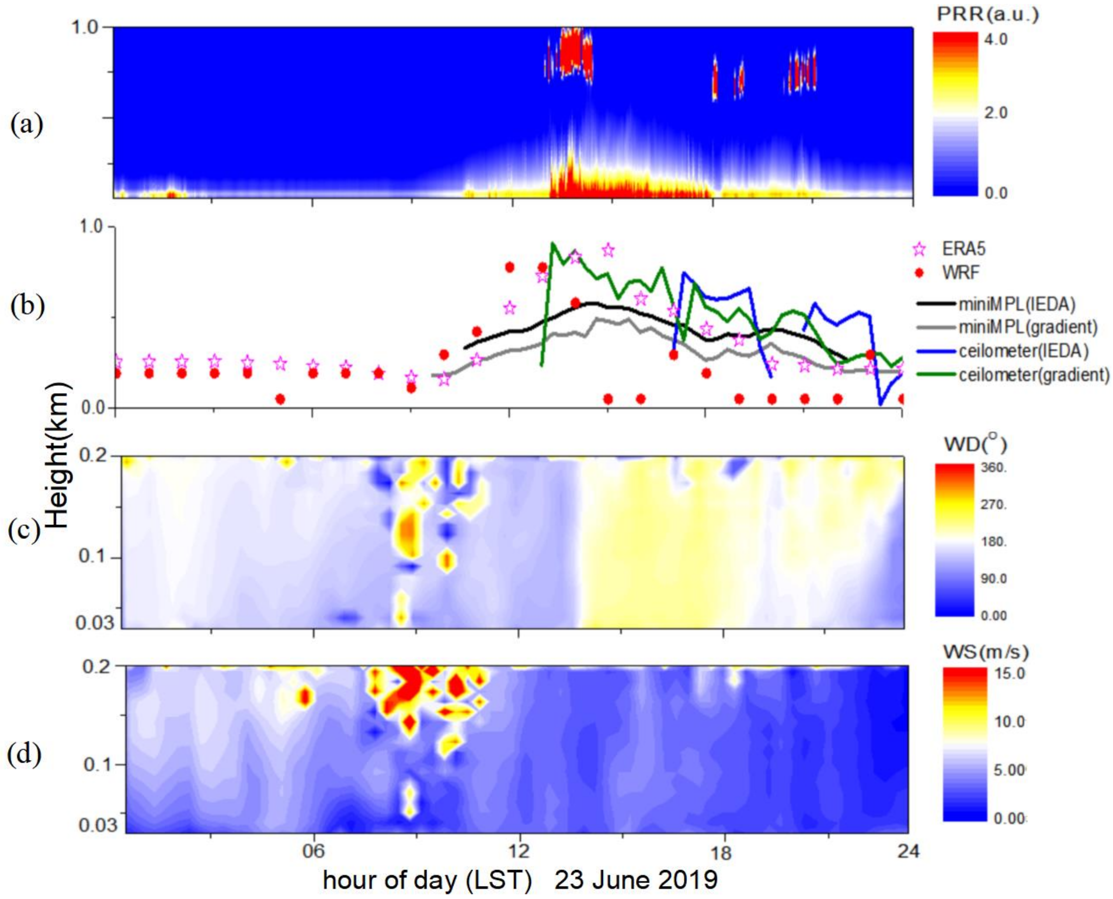

Figure 11. The same as Figure 10 except showing results from 23 June 2019.

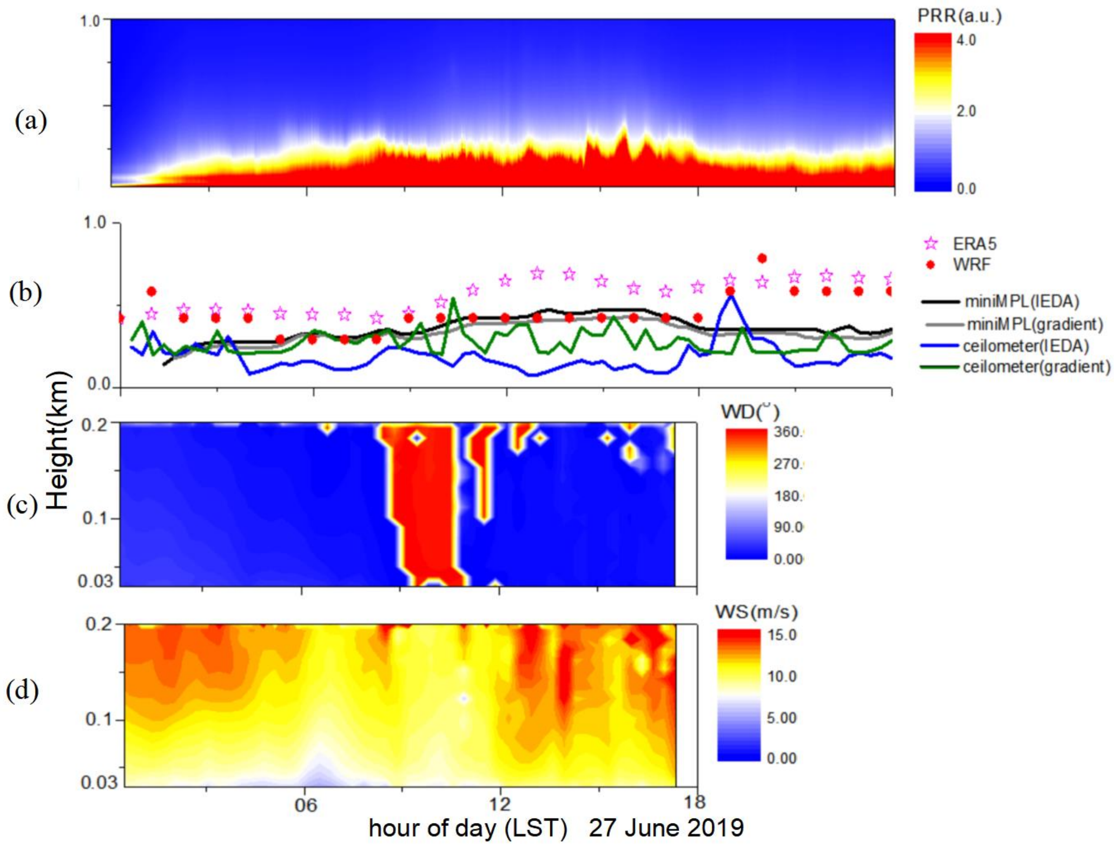

Figure 12. The same as Figure 10 except showing results from 27 June 2019.

2.The comparison of the two algorithms is superficial and the discussion of fig 3 (see below) is misleading. The IEDA gives smoother curves because I suspect it is designed to do so, but there is no evidence that it is 'better' than the gradient method.

Response: Compared to the gradient method, the IEDA is based on the continuous image instead of a single profile, therefore it can provide relatively smoother curves.

In the revised version, we checked and improved our IEDA by applying cloud removal and revising the process of the image conversion. Though it is not convincible to state that the IEDA is "better" than the gradient method for all instruments under all conditions (see our response to the main comment 1), it is robust for stable or unstable BLH detection on cloud-free days, especially when the SNR of the backscattered signal is high (i.e., miniMPL in our study).

The identification of cloud can be found in our response to the comment 3. Now we will explain our revision for the image conversion. In our initial implementation the gray conversion was applied to the colormapped image. In the implementation, we found that such conversion depends on which channel (red, green, or blue) of the image that the user has decided to use. However, none of the channel varies smoothly from black (0) through to white (255). Therefore, we improved the IEDA algorithm by making the conversion directly from lidar backscatter signal to gray value (0-255), in other words, producing a grayscale pseudocolour plot. The revised IEDA processing steps can be found as follows.

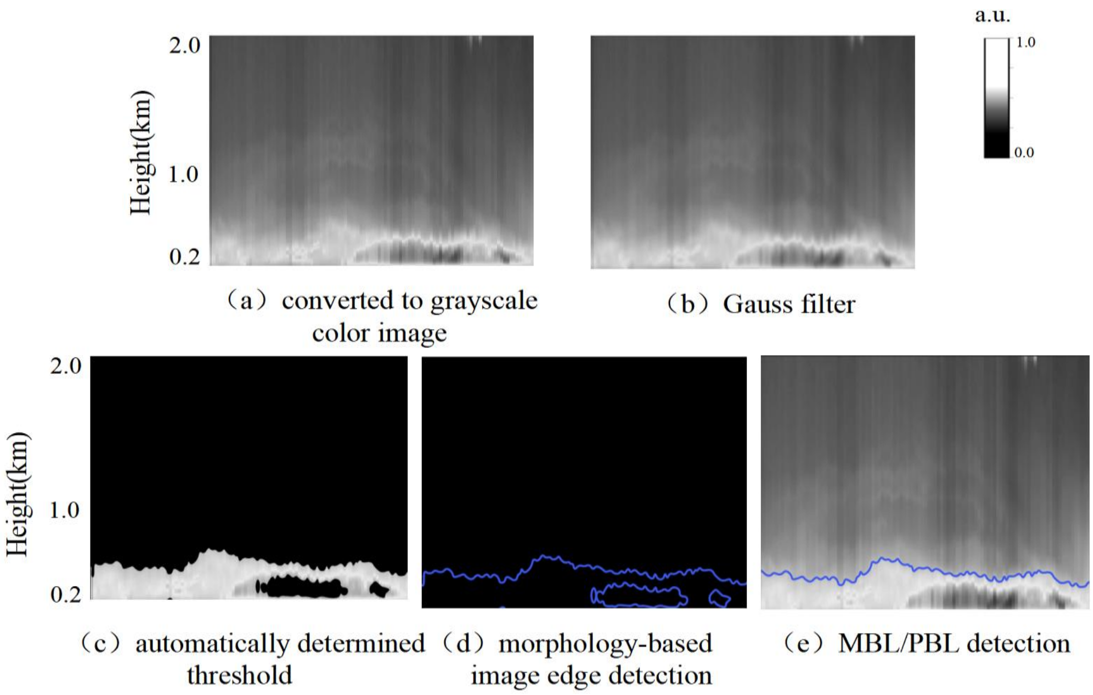

Figure 2. The main steps of IEDA processing for PBL/MBL detection.

Figure 2a: Converted to the gray image: We calculate and inverse the range-corrected lidar signal (PRR) to the 256-order gray color bar. Then we draw the gray image of the PRR, and take this image as the original image of morphological edge detection.

Figure 2b: Gaussian filtering: According to the gray values of the pixels to be filtered and their neighborhood points, the weighted average is carried out according to certain parameter rules. It can effectively maintain the image information filtering the superimposed noise. The specific operation step is to convolute the input image with two-dimensional Gaussian kernel, and take the convolution sum as the output pixel value. The output image is obtained after Gaussian filtering.

Figure 2c: Automatic determined threshold operation: According to the difference in gray characteristics between the target area to be extracted and its background, the image is regarded as a combination of two types of areas with different gray levels (target area and background area). The thresholds is automatically selected to determine a threshold interval. The pixels within this threshold range belong to the target area, while the pixels not within this threshold range belong to the background area. Thus, the corresponding binary image is generated.

Figure 2d: Morpholog-based image edge detection: Dilation and Erosion are two basic morphological processing operations that produce contrasting results when applied to either gray-scale or binary images. Among them, dilation is to add some pixels to the image boundary to make the image extend in the direction of increasing the gray index. In the contrary, erosion is to delete some pixels on the image boundary, so that the image shrinks in the direction of reducing the gray value. These two operations of corrosion and expansion can cause the greatest changes to the edge points. Based on this point, the corroded and expanded image is compared with the original image to obtain the point with the largest local change, that is, the edge point. Connecting these points and hence the whole edge of the image can be obtained.

Figure 2e：MBL/PBL detection: In order to make the detection more accurate and faster, the detection height is limited to below 2 km. Some isolated and unconnected edges are also eliminated manually. Finally, the actual value of the MBL/PBL can be obtained by simply calculating the position coordinates of the target edge in the image.

3.The effect of clouds on BLH measurements is barely mentioned, other than to state without proof that the IEDA method is better in this regard.

Response: Yes, low cloud layers impede the detection of the BLH. In our initial results, we found that the IEDA and gradient method will mistakenly identify the large gradient of the low cloud layers as the BLH. Specifically, the gradient method typically found the BLH at the beginning of the large negative gradient (base of the cloud layer), while the IEDA calculated the BLH slightly higher than the gradient method. Differences between these two methods were found to reach the maximum of 0.5 km. Therefore, we improved our algorithm firstly by cloud removal.

Cloud removal:

First, we used the gliding method to identify clouds. According to the characteristics of the cloud backscattered signal (Zuev et al.,1987; Cadet et al., 2005), it can be known that the integral of noise is close to 0, while in the area where the cloud exists, the signal integral value will be a considerable positive one. Therefore, the signal integral in the cloud can be very different from that in other cloudless areas, which can help effectively distinguish the cloud signal from noises. As shown in the following figure, a filtering window W is presented. W_h and W_L are the upper and lower edges of the window respectively to integrate the echo signal in the window, i.e

$$C(w) = \int_{W_L}^{W_H} X(z)\,dz \tag{1}$$

$$= \int_{W_L}^{W_H} (P(z) + v(z))z^2 dz = \int_{W_l}^{W_H} P(z)z^2 dz + \int_{W_l}^{W_H} v(z)z^2 dz \tag{2}$$

$$= \int_{W_L}^{W_H} P(z)z^2 dz \tag{3}$$

Where C(w) is the integral value of window W, and X (z) is the range-corrected signal. C(w) value approaches 0 in a certain interval if noises exist. For clouds, the integral value C(w) will be significantly larger than that of the aerosols. By properly selecting the threshold C(w), the cloud information can be extracted through the window integral value.

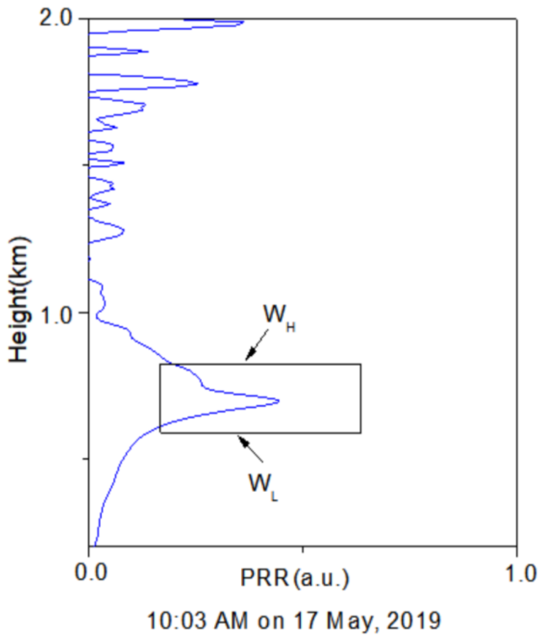

Figure. The cloud identification by sliding window integral algorithm window.

Furthermore, in order to ensure that all clouds within the measurement range are extracted, the window starts to move from the ground to the maximum detected height. Every time the window moves to a new area, the backscattered signal of the area is integrated to determine whether there is a cloud. If a cloud is present, further calculation of the position of the cloud base and cloud top will be implemented. Next the window continues to move upward from the cloud top until the signal ends. Because the inversion of cloud information is estimated by the movement of the window and the integral calculation of the signal in the window, this algorithm is called sliding window integral algorithm. We then identify the BLH after discarding the detected cloud profiles.

Revised Figure 3

The revised Figure 3 below shows the BLH retrieval from ceilometer and miniMPL against ERA5 reanalysis data under cloudy conditions. For the miniMPL, the IEDA (green line in Figure 3a) accords better with ERA5(magenta star) and provides fewer variable results compared to the gradient method (black circle in Figure 3a) as expected. For the ceilometer, the gradient method (black circle in Figure 3b), in the contrary, outperforms the IEDA (green line in Figure 3b), with the latter overestimating the BLH significantly compared to the ERA5 BLH. It is possibly because the IEDA fails to distinguish the target area and background area due to the low SNR of the ceilometer. These results are similar to the our statistical BLH analysis in our response to comment 1. We also list several reasons for this significant discrepancy between miniMPL/ceilometer and ERA5 BLHs in that response. Among them, we believe the presence of the clouds contributes the most under cloudy conditions, though other reasons (i.e., different definition of BLH, coarse resolution of ERA5) are not to be ruled out.

The Figure 3 shows that the detection of the BLH under the presence of clouds remains challenging. Again, no single method can provide adequate solutions for BLHs identification under all conditions. We would recommend for the BLH retrieval under cloud-free days and more specifically IEDA for the miniMPL and gradient method for the ceilometer. More detailed statistic and case analysis can be found in the section 3.1 and 3.2.1 of the revised version.

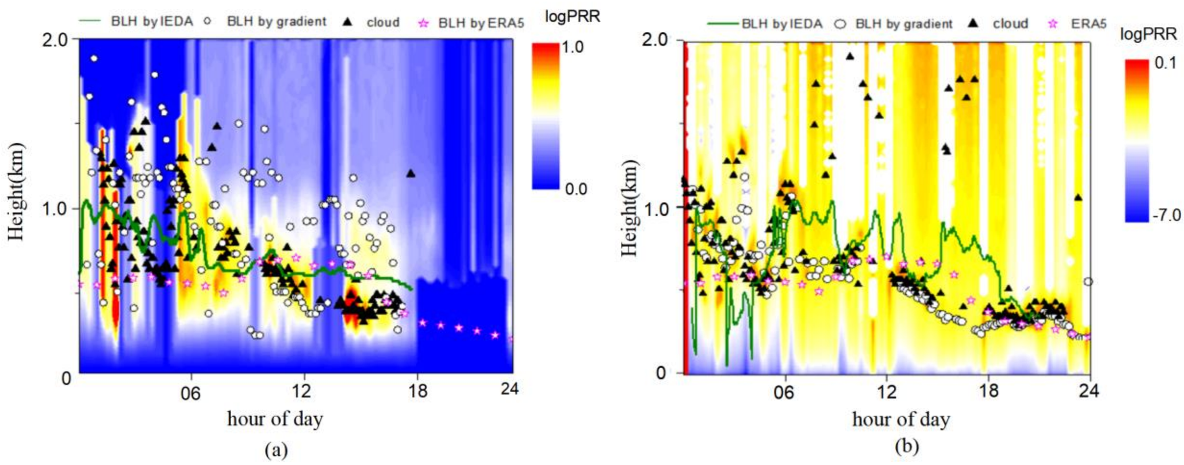

Figure 3. BLH estimations derived from (a) miniMPL and (b) ceilometer on 17 May 2019 (LST)

The heights in all panels are in km AGL. The vertically aligned color bar (on a linear scale) on the right indicates the intensity of range-corrected signal in arbitrary units (a.u.). Solid green lines and black circles indicate the BLH estimations using IEDA and gradient method, respectively. The magenta star indicates the 1-h averaged BLH results from the ERA5 reanalysis data. The clouds are marked with black triangles.

4.The result that DPR for pure oceanic air masses is lower than that for a continental air mass with a dust component is hardly new.

Response: Yes, the particle linear depolarization ratio (PLDR) only acts to verify the continental sources in the episode 3 (E3). Besides evaluating the IEDA and gradient methods for BLH identification using miniMPL and ceilometer, another object of our study it to analyze the different characteristic of MBL and aerosols suspended in the layer. Episode 3 presents the stable boundary layer characteristic under the continental sources and the relatively higher PLDR could validate it. Besides that, we also include the radon concentration in Figure 6d to prove it.

For this paper to be publishable, the authors must decide what scientific story they want to tell and structure their paper accordingly. I'm aware that this is a measurement report, but even so the standard of presentation falls well below what is expected, and the relevance of the measurements to atmospheric science generally (rather than locally to Cape Grim) is not explained.

Response: Thank you for the suggestion.

The main objective of this measurement includes two parts. Firstly, in order to evaluate the newly-developed IEDA for BLH retrieval, we review various methods (IEDA and gradient method) across a miniMPL and a Vaisala CL31 ceilometer located in a costal environment. These BLHs are then compared to ERA5-derived BLHs to arrive at the automated algorithm with the least manual inspection required. The effect of cloud signals on the BLH retrieval is also observed in both retrieval methods in this study. Though no single approach can resolve clouds and provide trustworthy BLH under all condition, distinct methods are recommended for different instrument. More specifically, the IEDA are more suitable for miniMPL whose aerosol backscattered intensity is relatively strong while the gradient method could provide more trustworthy BLH for the ceilometer.

Secondly the Southern Ocean is a particularly interesting region for boundary layer observations. Though various campaigns have been implemented to study the MBL and aerosol properties, the temporal and spatial resolution of conventional meteorological information and the influences of marine/continental sources on the boundary layer evolution are still scarce. In addition, the different characteristic of MBL evolution from BL (boundary layer) over land should be expected, "*The BLH is essentially a thermodynamic concept, but the marine boundary layer can be stable, inhibiting the vertical transport of aerosol"*, as you mentioned before. However, owing to the observing site located at the height of a cliff 94 m above mean sea level, the MBL we observed suffers less coastal impact than pure coastal sites in westerly sector baseline. For example, considering the low BLH (confined to less than 1 km) in our study, the decoupling trend of the MBL (Luo et al., 2016) was not observed during the campaign. Furthermore, the MBL was characterized with a typical diurnal structure under the marine sources, which is similar to the BL evolution over land. The growth of the convective boundary layer in our two events was also highly associated with the changes in surface temperature and wind speed profiles. In contrast, the MBL tends to be well mixed and stable under the strong continental sources. These results indicate that the MBL near the coastal region in Cape Grim may be more associated with relatively small fetches to mesoscale advection. And the continental sources could also significantly influence the MBL evolution.

In summary, the main goals of the present study are (1) to evaluate the feasibility of IEDA-derived BLH for the miniMPL and the ceilometer (2) to investigate the impact of different sources on the boundary layer evolution in the coastal region. This study aims to depict the spatial-temporal structure of BLH variability in winter Cape Grim, thereby complementing the spatial and/or temporal details of vertical BLH and wind information observational studies that is scarce in the Southern Ocean.

We have clarified the objective of this measurement in the last paragraph of the “Introduction” part.

Detailed comments (major)

1.The authors present in fig.3 a derivation of the BLH using the IEDA and gradient methods for 17 May 2019, concluding that the former method is best for the lidar and the latter for the ceilometer. I find this conclusion difficult to reconcile with the figure. Taking the left-hand panel, the BLH is around 0.7 km from 3 to 12 h, falls to around 0.4 km by 15 h where it remains for the next few hours, before rising to a maximum around 0.5 km at 21 h and falling sharply to around 200 m at 24 h. The IEDA data, where shown, are consistent with the circles on the left-hand panel. Contrast this with the right-hand panel, where the IEDA line from 6 – 12 h is around 0.8 – 0.9 km, gently falling to around 0.7 km by the evening. This is almost twice the height from the ceilometer!! Furthermore, many of the circles on the right-hand plot (notably between 14 and 18 h) are consistent with those on the left-hand plot. The authors do not even comment on this discrepancy, and based on this evidence I conclude that they do not have a reliable method of deriving BLH from their data.

Response: Thank you for the comment. We have improved our BLH detection algorithm (both IEDA and gradient) and re-plotted Figure 3. Besides that, we have changed the color scale and log scale to make it more visible. See the “revised Figure 3” part of our response to the main comment 3.

2. According to the final sentence of p.5, the shaded period E1 in fig 5 contains a sea breeze, and E2 a ‘sea breeze and offshore interaction pattern’, whatever that is. It is not clear at all how the authors come to these conclusions – how do they define a sea breeze? A reference to Caicedo et al 2021 is given but surely the criteria are not that complex? Then on l.198, we are told that during E1 and E2 the wind speed varied from 4 to 12 m/s, which is not consistent with the diagram. In E1 the wind varies from 2 to 8 m/s and in E2 from 2 to 6. The peak of 12 m/s *occurs in the unshaded section between them, during westerly flow. During E3 the maximum wind speed in 5b is 12m/s, not 14 m/s as on l.200. On l.203 the wind vector is said to veer from SW to W from 20 to 23 June, but that isn't what is shown on 5a. Finally, the statement on l.208 that the ceilometer BLH were higher than the lidar BLH from 20-24 June is only true some of the time – at other times the ceilometer BLH is lower. Quite simply, this whole paragraph is inconsistent with the data presented and reflects carelessness on the part of the authors. Furthermore, it only becomes evident in section 3.2.3 why the periods E1, E2 and E3 were selected – this should be mentioned at the beginning of 3.2.*

Response: Apologies for the misleading presentation. The wind speed varied from 2(Yes, not 4) to 12 m/s from 20 June to 23 June, 2019. The maximum value of wind speed indeed appeared at 21:00 LST on 27 June, 2019. The wind vector varied from 145^{o}(SE) to 215^{o} (SW) through the day on 20 June. The wind direction fluctuated and reached the maximum value of 225^{o} (SW) at 15:00 LST in 23 June. Then the wind continuously veered to the southern direction until the morning of 24 June. We have checked the misleading presentation through the paper.

As for the order of subsections for section 3.2, we also have revised it as:

3.2.1 BLH evolution under different sources

3.2.2 Vertical distribution of MBL aerosols

3.2.3 Synoptic conditions

3.2.4 Backward trajectories

3. The interpretation in section 3.2.3 leaves much to be desired. For a start, it is repetitive and doesn't obviously make a point. E1 and E2 were periods of sea-breeze flow, so it is not surprising that the signal of land convection is seen as the air sloshes out to sea and back. On l. 244 the wind direction is said to change from SE to SW at 0900 on the 20th, which is simply not true – the change in direction is around 50°, not 90°, and the sodar shows a change to southerly (U=0). On l.247 a throwaway sentence attributes the overestimate of BLH in WRF to 'non-accurate prescription of surface roughness and induced turbulence', with no evidence at all. How did the 'weak sea breeze interact with the uplifted strong offshore wind' (l.250)? What does 'interact' mean here? On l.272 reference is made to lidar extinction – how was this measured? We've only seen backscatter mentioned up to now.

Response: Yes, there is one-hour gap when the wind direction changed from SE to SW. We have re-written the sentence as "Two hours later, the wind direction began to shift southerly from 09:00 LST and maintained SE from 11:00 LST to the rest of the day, which coincided with the sodar results."

Besides WRF, we have included the ERA5 reanalysis data and re-plotted the BLHs comparison in Figure 9,10 and Figure 11 (now presented as Figure 10,11 and 12). The significant discrepancy between miniMPL/ceilometer and ERA5 or WRF BLHs are possibly due to (1) the different definitions of the BLH applied to each method, (2) the stringent conditions for the WRF parameterization (Banks et al., 2015), (3) the coarse resolution of ERA5 and WRF, and the presence of the lofted layers. We have also stated that in the response to the comment 1.

The phrase of "weak sea breeze interacts with the uplifted strong offshore wind" has been removed.

For the aerosol extinction coefficient retrieval, the processing steps are as follows. After data pre-processing, including range correction, background subtraction, dead-time correction, AN and PC signal merging, and assumption of reference height in an aerosol-free region (usually the upper troposphere, here we chose the range of 7-8 km as the reference height according to the specific circumstance in every process of data analysis), the aerosol backscatter coefficient at 532 nm was inversed by the Klett method (Klett, 1981). According the previous measurements (Müller et al., 2007; Omar et al., 2009), the constant lidar ratio was assumed as 20 sr and 60 sr (at 532 nm) for marine and continental aerosols, respectively to obtain the aerosol extinction properties. We have added a new subsection 2.2.3 "Aerosol Extinction coefficient" to explain the retrieval method.

4.This is further compounded in 3.2.4 by a complete section on extinction coefficient. What algorithm was used to derive it? The backscatter signal does not give the aerosol backscatter coefficient (and hence the extinction coefficient by the assumed lidar ratio) directly. BLH may be derived from the signal profiles, but extinction coefficient requires a retrieval (as indeed is mentioned on l.288).

Response: Please see the last paragraph of our response above.

Detailed comments (minor)

1.p.4 l.120 and fig.2. More details are required of the IEDA algorithm as it is not possible to reproduce this study from the description given. For a start, axes and axis labels are needed in Fig 2 so that we can see the scales being discussed. Secondly, the colour scales should be shown, especially the grayscale in panel b where the white colour seems to correspond to an *intermediate value of backscatter (why?). Thirdly, explain better how you go from 2b to 2c – a Gaussian kernel smooths a plot and you take a difference between this and the original plot in some way but I'm not sure how. I realize you give a reference to Xiang et al, but this paragraph needs to be clearer. And do you really mean 'corrosion' on line 124?*

Response: We have revised the paragraph to make the IEDA algorithm more precisely. The improved procedure of IEDA and the revised Figure 2 can also be found in our response to the main comment 2.

Thank you for pointing out the "corrosion" and it has been corrected as "erosion".

2.p.4 l.133 I can't see any green circles in fig 3b, though I can see a lot of scatters in the gradient method

Response: Figure 3 has been re-plotted and can be found in the "revised Figure 3" part of our response to the main comment 3.

3.p.6 l.222. You haven't analyzed the characteristics of aerosols; you have used a trajectory model to calculate the source region of the air masses that passed over Cape Grim.

•l.226 period

•l.238 the nocturnal BLH is more like 200 m

Response:

We have added more details about the characteristics of aerosols in the section 3.2.2.

We have corrected the word" period".

We have re-plotted the Figure 9, 10 and 11 (now presented as Figure 10, 11 and 12 in the revised version). In the 20 June case, the mean nocturnal BLH from 18:00 to 23:00 LST calculated by miniMPL(IEDA), miniMPL(gradient), ceilometer (IEDA) and ceilometer (gradient) are 0.32 km, 0.22 km, 0.62 km and 0.52 km, respectively. For comparison, the nocturnal BLHs from ERA5 and WRF model are 0.71 and 0.48 km, respectively. We have re-rewritten the related statement.

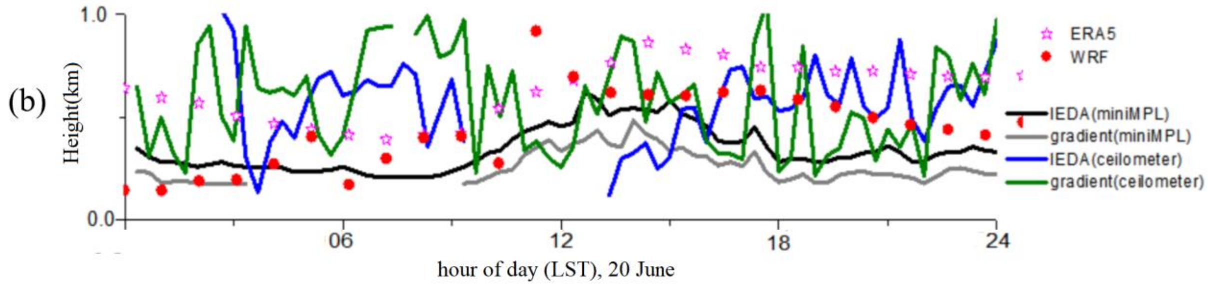

Figure 10b. BLHs comparison from miniMPL and ceilometer against EAR5 and WRF on 20 June, 2019.

4.p.7 l.239 what is special about 0900? The change of wind with height is no different to the preceding 9 hours; if anything it is less

Response: In order to make the plot easier for readers and reviewers, we have re-plotted the wind information chart by showing wind vector (direction and speed) plot rather than two separate zonal & meridional contours. For the revised wind vector on 20 June 2019, the wind direction shifted to southerly with height at 09:00 LST. Then it slightly varied between 160^{o} to 180^{o} (SE to S) in the next three hours. It shifted to the SE completely at all heights from 12:00 LST and maintained the SE in the afternoon. At night it varied back to the southern direction. For the wind speed, it increases with the height, ranging drastically from 2.2 m/s up to 15.1 m/s from 00:00 to 09:00 LST. After 09:00 the wind speed varied more leisurely with the height from 1.6 to 5.7 m/s until 13:00 LST. Therefore, the changed wind speed and shifted direction from 09:00 LST could indicate the onset of MBL development.

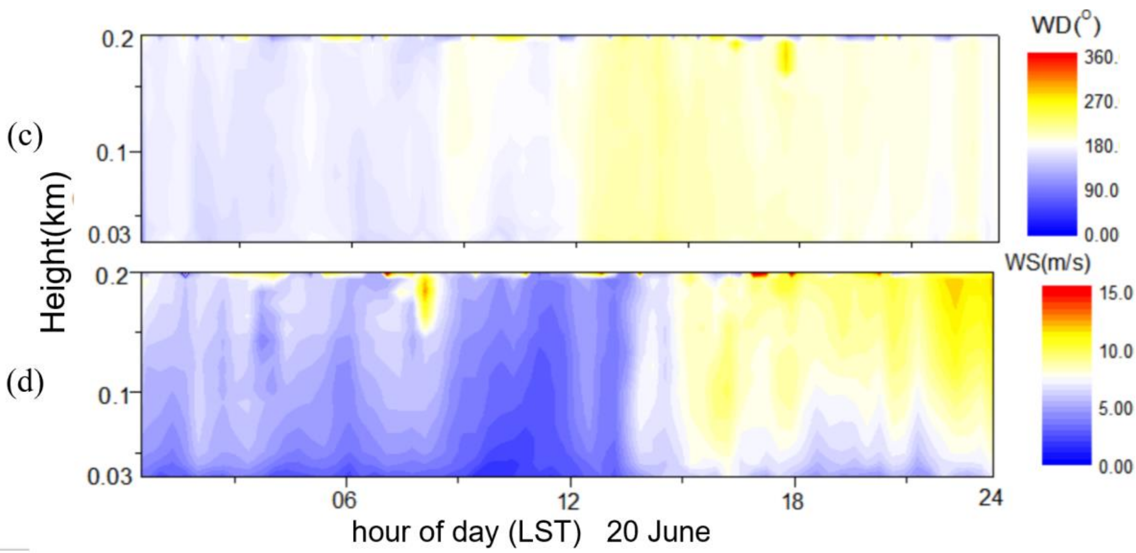

Figure 10c and 10d. Wind direction and wind speed on 20 June, 2019.

5.p.7 l.259 why is the low-level jet baroclinic? The front is nowhere near Tasmania.

Response: We have removed the phrase.

References

1. Banks, R. F., Tiana-Alsina, J., Rocadenbosch, F., and Baldasano, J.M.:Performance evaluation of the boundary-layer height from lidar and the Weather Research and Forecasting model at an urban coastal site in the North-East Iberian Peninsula, Boundary-Layer Meteorol., 157, 265-292, 10.1007/s10546-015-0056-2, 2015.

2. Cadet, B., Giraud,V., Haeffelin, M., Keckhut, P., Réchou, A. and Baldy, S.: Improved retrievals of the optical properties of cirrus clouds by a combination of lidar methods, Appl. Optics, 44(9):1726-34, DOI: 10.1364/AO.44.001726, 2005.

3. Klett, J. D., Stable analytical solution for processing lidar returns. Appl.Optics, 20:21,1981.

4. Luo, T., Wang, Z. E., Zhang D. M., and Chen, B.: Marine boundary layer structure as observed by A-train satellites, Atmos. Chem. Phys., 16, 5891–5903, 2016.

5. Müller, D., Ansmann, A., Mattis, I., Tesche, M., Wandinger, U., Althausen, D., and Pisani, G.: Aerosol-type-dependent lidar ratios observed with Raman lidar, J. Geophys. Res.-Atmos.,112, D16202, https://doi.org/10.1029/2006JD008292, 2007.

6. Vladimir E. Zuev, G. M. Krekov, M. M. Krekova, and Titov,G.A.: Mean characteristics of lidar signals from broken clouds, Appl Optics，26(15)：3018-30,1987, DOI: 10.1364/AO.26.003018